

Advances in Singly-Connected Closed Field Line Plasma Devices and Extrapolation to POP Level Experiments and Reactors

A.L. Hoffman, L.C. Steinhauer – *University of Washington, Seattle, WA, USA*

H. Ferrari, R. Farengo – *Centro Atomico Bariloche, S.C, de Bariloche, Argentina*

ABSTRACT

Recent advances in creating stable, hot, steady-state field-reversed-configuration (FRC) plasmas using rotating magnetic fields (RMF) have made this an appropriate time for re-examining the old field-reversed-mirror (FRM) concept. The reactor advantages of such a linear, naturally high beta configuration would be enormous, but previous attempts to produce field reversal using tangential neutral beam injection (TNBI) alone were unsuccessful. Simple scalable extensions of present RMF produced FRCs can result in ideal traps for TNBI produced energetic ions, and detailed calculations show high efficiencies of TNBI production of energetic ion rings within such FRCs. If non-standard MHD effects such as strong flow and highly energetic ions are able to extend FRC stability to larger sizes, then the principal need will be to reduce present high values of anomalous cross-field resistivity. Experimental trends show how this may be achieved, and the present experimental and theoretical status of the most basic issues of FRC stability, confinement, and current drive are summarized, along with the new calculations on TNBI. The parameters for a modest sized ‘proof-of-principle’ device which can address these basic issues, as well as provide enough flux for efficient TNBI trapping, are given.

1. INTRODUCTION

The desirability/necessity of closed magnetic field lines for successful plasma confinement has long been recognized. Simultaneously, the overwhelming advantages of a linear, singly connected geometry are obvious. In the past three decades experiments in the U.S., Russia, and Japan have made steady progress toward combining these features, i.e. in developing closed field line singly connected plasma traps within a cylindrical-like vacuum vessel. Present day experiments, on the order of 1 m in diameter, have achieved quasi-steady plasmas with temperatures of 100-200 eV at densities of the order of 10^{19} m^{-3} , which are completely stable. Simultaneously, theoretical understanding of these systems has advanced. In this paper we summarize this progress and examine the basic issues relevant to such closed field line linear systems as fusion reactors. We also develop scaling relations for extrapolation from present experiments to a next step, Proof of Principle (POP) level device, which would go a long way toward resolving these issues.

Attempts to combine closed field lines with linear geometries began with the unsuccessful Astron program[1] and continued with a less well known part of the early mirror program, the field reversed mirror (FRM).[2] Mirrors have been pursued vigorously in the past, and are still being investigated to some extent due to the recognized engineering advantages of linearity. With the addition of multipole fields, or Ioffe Bars, claimed physics advantages are good

stability at high beta and possible near-classical radial confinement.[3] However, the necessity to ‘plug’ the ends to avoid high thermal losses has led to the complex and costly tandem mirror approach.[4,5] At the time of the initial mirror investigations, the tandem mirror was only one of two proposed ‘Q-enhancement’ schemes, the other being the FRM. In order to produce a FRM, the azimuthal currents need to be high enough to reverse the interior field lines, which has the added advantage of yielding a very high average beta (between 0.5 and 1.0 for an elongated plasma). The approach of forming FRMs using tangential neutral beam injection (TNBI) was investigated at Lawrence Livermore National Laboratory (LLNL) on the 2XIIB facility.[6] However, while the central magnetic field could be greatly reduced, forming moderate average beta plasmas, field reversal was not realized, and the attempts were abandoned. Moderate beta diamagnetic plasmas can be formed by simple heating alone, but there are several reasons why the change in magnetic field topology brought on by field reversal could not be achieved with slow tangential neutral beam addition.

The Astron program attempted to produce field reversal through the slow build-up (short successive pulses) of a high current electron ring. Although this was unsuccessful, probably for reasons related to the lack of success in the 2XIIB experiments, field reversing electron rings were produced by Prof. Hans Fleishmann at Cornell University using fast injection of energetic electrons.[7] However, attempts to accomplish the same thing with ion beams, which would be required for practical fusion, were unsuccessful.[8] Field reversal was then pursued in high voltage theta-pinch through trapping some initial reverse bias field, which then reconnected with a rapidly applied forward field.[9] This method of producing field reversal with diamagnetic currents was very successful, and the resulting topologies were named field-reversed-configurations (FRC). Due to the extremely high input power (several GW) it was easy to produce high density, hot plasmas, but the poloidal flux levels were low (1-10 mWb) and there was no means available for either building up or sustaining the flux. For reactors, these theta-pinch formed FRCs were only suitable for subsequent compression and pulsed fusion.

A more reactor relevant FRC formation method, which is also capable of building up and sustaining the poloidal flux, is rotating magnetic fields (RMF). RMF had been explored as a current drive method [10] and was developed over several decades in a long series of rotamak experiments by Prof. Ieuan Jones at Flinders University.[11] The RMF, if at a frequency intermediate between the electron and ion gyrofrequencies, drives an azimuthal electron current in the same manner as an induction motor drives a rotor. The rotamak experiments were successful in forming and sustaining (for up to the 40 msec timescale of their power supply) spherical FRCs, but the plasmas rested against the glass walls of the vacuum vessel, and were cold and generally not even fully ionized. The RMF technique was adapted to form and sustain standard prolate FRCs in the cylindrical TCS (Translation, Confinement, Sustainment) experiment at the University of Washington, where the main improvement was the use of a flux conserver to keep the plasma off the plasma tube walls.[12] This experiment also had problems

reaching plasma temperatures above a few tens of eV due to the generic difficulty of overcoming initial radiation barriers when creating high beta plasmas with low input powers. However, recent success in an upgraded version of TCS, called TCSU, using modern high vacuum and glow discharge cleaning techniques to surmount these radiation barriers and achieve temperatures well over 100 eV, has opened up an exciting opportunity for realizing the reactor benefits of the FRM, or FRC.[13]

The TCSU experiments have elucidated many aspects of steady-state FRC physics and RMF current drive, which are summarized in Section 2. In particular, the observed cross-field resistivity scaling with electron drift velocity is of critical importance in realizing a particular claim for quasi-linear systems of near classical confinement. The RMF itself has also provided the same stabilizing properties to radial interchange modes as demonstrated using multipole fields.[14] Tangential neutral beam addition has not been part of the TCSU or any RMF program due to cost and size constraints, but should be an integral part of further steady-state FRC/FRM development now that a technique exists for forming the hot, low density FRCs which would be ideal traps for energetic charge-exchange ions. TNBI would naturally complement RMF in heating and flux sustainment, while also providing a momentum source in the opposite direction to allow control of azimuthal velocity profiles. High energy ion ring components and velocity shear are calculated to be important in providing stability to axial modes, stability which may not be realizable for larger FRCs with RMF drive alone.

The critical questions for FRC/FRM physics are the same as for any magnetic fusion geometry; 1) stability, 2) required power for current, or flux, drive, and 3) energy confinement. Technical questions such as exhaust handling and tritium inventory, which should be enormously helped by the linear geometry with a natural unrestricted divertor, are not treated in this paper. The three

Table 1
FRC Parameters

Parameter	TCSU $B_\omega = 5 \text{ mT}$ $85 \mu\Omega\text{-m}$	'POP-level' $B_\omega = 10 \text{ mT}$ $120 \mu\Omega\text{-m}$ $30 \mu\Omega\text{-m}$		'Reactor' $\sim 1 \mu\Omega$
$\langle \eta_\perp \rangle =$				
f_ω (kHz)	150	30		10
r_s (m)	0.37	0.9	0.9	2.0
B_e (T)	0.03	0.06	0.12	1.3
ϕ_p (Wb)	0.0035	0.045	0.090	4.5
T_i, T_e (keV)	0.12	0.32	0.65	10
n_m (10^{20}m^{-3})	0.1	0.15	0.3	2.0
s	1.0	3.0	4.2	22
λ_{ii} (m)	25	150	300	10,000
ρ_{ci} (m)	0.06	0.04	0.03	0.013
$\gamma_d = v_{de}/v_{ti}$	2.3	0.77	0.54	0.10
E_{ic} (keV)	0.6	18	72	24,000

critical physics questions, including the contributions of both RMF and TNBI, are discussed in Sections 3 through 5. To aid in this discussion parameters are listed in **Table 1** for current TCSU plasmas, a POP-level device which embodies a methodology for answering the critical questions, and for an idealized minimum size reactor (or more appropriate, a burning plasma experiment, FRC-BPE). (The various parameters are defined in the relevant sections.) Calculations are shown in Section 6 relevant to TNBI for the POP level device, and for TNBI and fusion-reaction-produced fast ion currents for the D-T reactor parameters. The unique ability of the POP-level device for addressing the above critical questions is summarized in Section 7, along with the overall promise and physics requirements for the FRM/FRC concept at reactor dimensions.

2. TCSU EXPERIMENTS & RMF CURRENT DRIVE SCALING

A Field Reversed Configuration (FRC) is simply a compact toroidal plasma (CT), usually elongated in the axial, z , direction, with little or no toroidal field. Its basic geometry is sketched in **Fig. 1** with r_s the separatrix radius and ℓ_s the separatrix length. If moderately elongated and confined inside a flux conserver of radius r_c , its

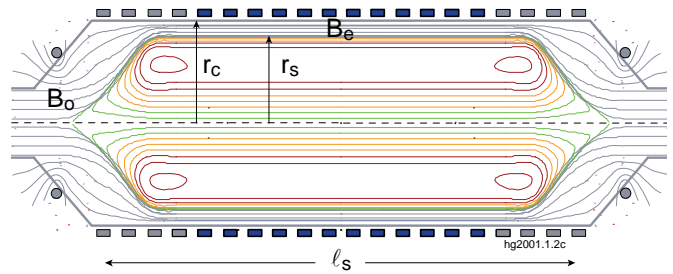


Figure 1. FRC geometry inside flux conserver.

external magnetic field is $B_e = B_0/(1-x_s^2)$, where B_0 is a bias field (either initial or increasing during flux build-up) and the dimensionless separatrix radius $x_s \equiv r_s/r_c$ is a key FRC parameter. Radial equilibrium is given by $p(r) + B_z^2(r)/2\mu_0 = B_e^2/2\mu_0$, and a simple examination of Maxwell's stress tensor determines an axial equilibrium constraint, $\langle \beta \rangle = 1-x_s^2/2$ [15]. The average β value for an elongated FRC must thus be ≥ 0.5 . A field null, $B_z(R) = 0$, exists at radius $R = r_s/\sqrt{2}$, and the amount of poloidal flux is constrained to $\phi_p = (x_s/\sqrt{2})^{1+\epsilon}\pi R^2 B_e$, with ϵ between 0 and 1 and generally about 0.3 for a typical Rigid Rotor (RR) current distribution (description in Section 4). FRCs formed by theta-pinch methods have generally had x_s values ≤ 0.5 and fairly high separatrix densities, but RMF formed FRCs tend to have $x_s \sim 0.8$, very low separatrix densities, and relatively more insulating flux.

RMF current drive works through the azimuthal forces exerted on the electrons by the RMF as long as the electron rotational frequency ω_e is less than the RMF frequency ω . In its simplest terms the RMF can be thought of as 'dragging' the electrons, much in the same manner as an induction motor drags a metal rotor. In a diamagnetic plasma the current arises simply due to a pressure gradient, and it is really poloidal flux that must be created and sustained. This requires an azimuthal electric field, E_θ , greater than or equal to zero. Simple, non-field reversed mirror

plasmas can be maintained by the $v_{er}B_z$ diffusive term in Ohm's Law through particle and heat addition, but this process is insufficient in a field reversed plasma where $B_z(R) = 0$.

A simple form of Ohm's Law in the azimuthal direction for a cylindrical plasma is

$$E_\theta = \eta_\perp j_\theta + v_{er}B_z + \langle -V_{ez}B_r \rangle . \quad [1]$$

(V_{ez} and B_r are oscillating quantities produced by the RMF, while the remaining terms are quasi-steady.) Poloidal flux build-up/sustainment in a compact toroid requires making E_θ greater than/equal to zero everywhere, where we take B_z positive outside the field null and j_θ is thus negative. RMF drives current, or produces flux, through the in-phase oscillations $\langle -V_{ez}B_r \rangle$. It is primarily the electrons that are driven for the normal case where $\omega \ll \omega_{ce} = eB_\omega/m_e$ and $\omega > \omega_{ci} = eB_\omega/m_i$, where B_ω is the amplitude of the RMF (it is actually the B_r component of the RMF, which is much less than B_ω for normal partially penetrated RMFs, which is relevant in these relationships). Various mechanisms, such as refueling and open field line end shorting prevent eventual excessive ion spin-up in present experiments.

An integration of Ohm's Law with a reasonable profile of $E_\theta(r)$ gives the equation for poloidal flux build-up (defining $\phi_p = -\int_0^R 2\pi r B_z dr$ since in normal notation B_e is taken positive).

$$\frac{d\phi_p}{dt} = 2\pi R E_\theta(R) = \frac{4}{\langle n_e \rangle e r_s^2} (\mathbf{T}'_{\text{rmf}} - \mathbf{T}'_\eta) , \quad [2]$$

where
$$\mathbf{T}'_{\text{rmf}} = \frac{2\pi r_s^2 B_\omega^2}{\mu_o} f(\zeta) , \quad [3]$$

and
$$\mathbf{T}'_\eta = 1.16\pi r_s^2 e n_m \left(\frac{B_e}{\mu_o} \right) \langle \eta_\perp \rangle . \quad [4]$$

\mathbf{T}'_{rmf} is the drive torque per unit length produced by an RMF of magnitude B_ω and \mathbf{T}'_η is the resistive torque per unit length calculated for a RR-type profile. η_\perp is the cross-field plasma resistivity, and $f(\zeta)$ depends on the ratio ζ of actual electron line current to the maximum possible RMF sustained line current,

$$\zeta = \frac{I'_{\text{line}}}{I'_{\text{sync}}} = \frac{2B_e/\mu_o}{0.5\langle n_e \rangle e \omega r_s^2} = \frac{\langle \omega_e \rangle}{\omega} . \quad [5]$$

Calculations show $f(\zeta)$ to be about equal to 0.1 for $0.2 < \zeta < 0.95$, and necessarily going to zero as ζ approaches unity.[13]

For ζ in the above range, $\omega_e \sim \omega$ near the FRC separatrix, while a region with $\omega_e < \omega$, whose depth and breadth depends on ζ , exists near the field null. Due to the near synchronous electron edge rotation, the RMF penetrates to near the field null, with the drive torque occurring principally between R and r_s (closer to R as ζ increases). The resistive torque per unit length \mathbf{T}'_η

is calculated for a rigid rotor type profile with uniform temperature, peak density n_m , and average resistivity $\langle \eta_{\perp} \rangle$. Equating the RMF and resistive torques, and using $B_e = (2\mu_0 n_m k T_t)^{1/2}$, where $T_t = T_e + T_i$ is the sum of electron and ion temperatures (assumed uniform), in steady-state the peak plasma density is

$$n_m (10^{20} \text{ m}^{-3}) = 1.4 \frac{B_{\omega}^{4/3} (\text{mT})}{T_t^{1/3} (\text{eV}) \langle \eta_{\perp} (\mu\Omega - \text{m}) \rangle^{2/3}} . \quad [6]$$

For typical TCSU conditions of $B_{\omega} = 5 \text{ mT}$, $T_t = 200 \text{ eV}$, and $\langle \eta_{\perp} \rangle = 100 \mu\Omega\text{-m}$, the peak plasma densities are about 10^{19} m^{-3} . The density is mostly determined by the RMF magnitude and the average cross-field resistivity, and is only weakly dependent on the plasma temperature, but in earlier TCS radiation dominated experiments with temperatures 5 to 10 times lower, typical densities were almost twice as high, in agreement with the Eq. (6) scaling. [16]

Using the above expressions, a useful relationship for scaling and evaluating experimental data is

$$\frac{B_e}{B_{\omega}} = 8.3 \frac{(T_t/n_m)^{1/4}}{\langle \eta_{\perp} \rangle^{1/2}} \quad [7]$$

where units of mT, eV, 10^{20} m^{-3} , and $\mu\Omega\text{-m}$ will be used henceforth in discussing experimental results for magnetic field, temperature, density, and resistivity. A numerical result for the power absorbed per unit length due to the azimuthal currents is

$$P' (\text{W/m}) = 10.8 \langle \eta_{\perp} \rangle B_e^2 . \quad [8]$$

The absorbed power due to resistive dissipation is independent of plasma radius for a given magnetic field since a larger area is compensated by a lower current density. Experiments have shown that the resistivity is much higher near the outer edge of the FRC, presumably due to the higher electron drift velocity there, [17] and if inner and edge resistivities are specified as η_i and η_e , the average resistivities to be used in the torque based and power based expressions are $\langle \eta_{\perp} \rangle_t = (0.73\eta_i + 0.27\eta_e)$ and

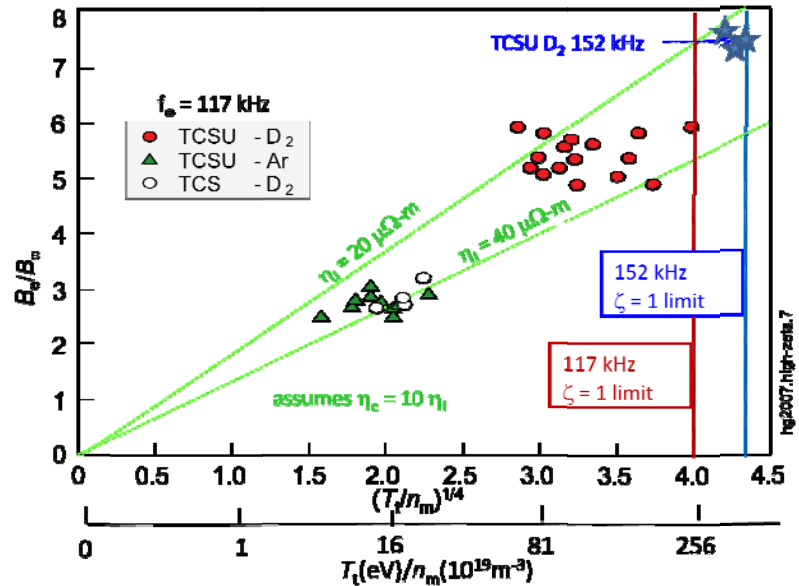


Figure 2. Measured ratios of poloidal field to applied RMF. (n_m given in units of 10^{19} m^{-3} for this figure.)

$\langle \eta_{\perp} \rangle_p = (0.58\eta_i + 0.42\eta_e)$. η_e has a greater effect on the power absorption, which is proportional to the square of the current density. We use a value of $\eta_e = 10\eta_i$ which best fits all aspects of experimental data, and generally list the values of η_i .

In reference to Eq. (7), the ratio B_e/B_{ω} is plotted in Fig. 2 as a function of $(T_t/n_m)^{1/4}$. Results are shown for both TCSU and TCS, and for some TCSU experiments run in Argon to illustrate that the difference between TCS and TCSU was indeed due to the lowering of impurity and radiation levels. Lines are drawn representing different values of the inner resistivity in accordance with Eq. (7). The absorbed power which is needed to sustain the FRC flux is obviously an important quantity.

This is plotted in Fig. 3 as a function of B_{ω}^2 since for low ratios of B_e/B_{ω} , most of the power absorption appears to occur simply due to the presence of the RMF, which probably indicates a type of kinetic wave absorption. By looking at the absorbed power difference when B_e is increased, an expression for the absorbed power in the TCS/TCSU experiments can be derived:

$$P'_{\text{abs}} (\text{W/m}) = 40 \times 10^3 B_{\omega}^2 (\text{mT}) + 1.2 \times 10^3 B_e^2 (\text{mT}) \quad [9]$$

Comparing the portion due to B_e^2 with Eq. (8) yields a value of $\langle \eta_{\perp} \rangle_p = 110 \mu\Omega\text{-m}$, or $\eta_i = 23 \mu\Omega\text{-m}$, about the same result as calculated from the torque analysis. The wave related power absorption is useful for initial plasma heating, but will become less important, at least based on Eq. (9), as the ratio B_e/B_{ω} increases, as it must to approach reactor parameters.

The TCSU results in Table 1 were obtained in deuterium with an RMF B_{ω} value of 5 mT. (Only the total temperature T_t has been measured so far, but all indications are that T_e is somewhat larger than T_i . $T_i = T_e$ is assumed in the table.) The values of $\langle \eta_{\perp} \rangle$ needed to achieve the listed n_m , T_t , and B_e values are based on Eqs. (6) or (7). The first column under the ‘POP-level’ label is based on achieving the same $B_e/B_{\omega} = 6$ ratio as obtained in TCSU assuming a larger RMF power supply with a B_{ω} magnitude of 10 mT. The values of T_t and n_m listed are consistent with pressure balance and $\zeta = 0.8$ in Eq. (5) for the listed RMF frequency, and the allowable average resistivity is even higher than experienced in TCSU due to the higher assumed ratio of T_t/n_m . The 45 mWb poloidal flux is more than sufficient for efficient TNBI, which

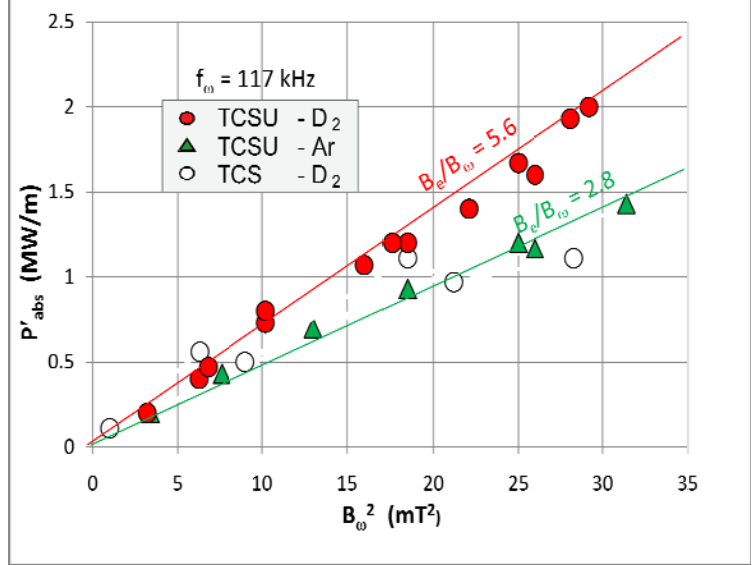


Figure 3. Absorbed powers in RMF sustained FRCs.

would be an important component of the POP-level device. The second column under the ‘POP-level’ label describes what would be obtainable if the resistivity were reduced by a factor of four to $\langle\eta_{\perp}\rangle \sim 30 \mu\Omega\text{-m}$, which would be necessary for the experiment to be a success. The meaning and importance of the other parameters, particularly the ratio of electron drift velocity v_{de} to ion thermal velocity v_{ti} , and the critical neutral beam injection energy, E_{ic} , are discussed in the following sections, where the ability to obtain the stipulated temperatures is also discussed. (The plasma density is directly dependent on the plasma resistivity in accordance with Eq. (6), which is a unique feature of RMF sustained FRCs. The temperatures listed in Table 1 were chosen somewhat arbitrarily, but even if they could not be achieved by RMF alone, the listed magnetic fields and poloidal fluxes, critical for TNBI, would only be marginally affected.) For good power balance in an FRM reactor, if it were driven solely by RMF, $\langle\eta_{\perp}\rangle$ would have to be reduced by over two orders of magnitude. It is expected that much of a reactor’s current would be self-driven by particle injection and reaction products, but we will show why we believe such low bulk resistivities to be possible in a larger, higher field device by reducing the drift parameter, v_{de}/v_{ti} , to below 1.

3. STABILITY

Simple mirror plasmas are subject to micro-instabilities arising from an anisotropic distribution function and interchange instabilities due to unfavorable curvature near the mirror ends. The former are not important for FRCs, or FRMs, but the latter are ubiquitous. A consideration of beta limits is not relevant for FRCs since they are, by definition high beta (due to low, if any, toroidal field). In most FRC experiments radial interchange instabilities are driven by plasma rotation and the accompanying centrifugal forces. The most common of these is the rotating $n=2$, which can be stabilized by multipole fields[18] or RMF[14] and has also been noted to be stable in translated FRCs which have moderate amounts of toroidal field.[19] Closure of the magnetic field lines at the ends leads to axial MHD instabilities due to the unfavorable curvature there. The most worrisome of these, and the most studied, is the $n=1$ tilt. This MHD instability of compact toroids (CT), either FRCs or spheromaks, was first pointed out by Rosenbluth and Bussac.[20] They found that prolate CTs were always MHD unstable since the tilt started out as an asymmetric axial shift (called the internal tilt), but that oblate CTs, whose tilt was external, could be stabilized by close fitting conducting walls. The latter calculation has governed all subsequent spheromak experiments, but most FRC experiments, either theta-pinch or RMF formed, have involved mildly to highly prolate plasmas. Contrary to simple MHD theory, it is these prolate FRCs that have experimentally proven to be the most stable. Recent merging spheromak experiments at Princeton Plasma Physics Laboratory (Merging Reconnection Experiment) and at Swarthmore University (Swarthmore Spheromak Experiment), annihilating oppositely directed toroidal fields, have formed FRCs in an oblate flux conserver which, although short-lived, have appeared stable.

The stability of prolate FRCs, indeed the robust stability in surviving violent formation dynamics in theta-pinches[21] and highly supersonic translation and reflection off mirrors with capture in magnetic wells,[22] has usually been attributed to their kinetic nature. The kinetic nature is most accurately represented by a parameter called s , equal to the radially weighted number of internal ion gyro-radii between the field null and the separatrix.

$$s = \int_R^{r_s} \frac{r dr}{\rho_i r_s} \quad [10]$$

Another related parameter, often used in theoretical work, is $S^* = r_s/(c/\omega_{pi})$, where the ion skin depth c/ω_{pi} is about equal to ρ_i for a high beta FRC. (S^* is about 5-10 times larger than s , depending on the internal flux profile.) The tilt growth rate, relative to the MHD growth rate, has been shown to decrease with large ratios of E/S^* , where $E = \ell_s/2r_s$ is the FRC elongation, which may make other effects on tilt stabilization more effective. Other theoretical work involves strong rotation, which is present in all FRCs.

A theta-pinch based FRC experiment, the Large s Experiment (LSX) was built to explore stability at high s values.[23] This 80-cm diameter experiment was only operated for one year (1991) due to budgetary decisions. Successful formation became more difficult at higher s due to the increasingly dynamic nature of the process, but this difficulty could be overcome through extreme care in making both the radial and axial implosions occurring during the formation process very symmetric. Long lived (~ 1 msec) FRCs were formed up to $s = 4$. Even higher $s \sim 8$ FRCs could be formed with various remaining asymmetries and shorter lifetimes, but there was no indication of the tilt instability.[24]

A kinetic theory of FRC stability is difficult since standard FLR expansion techniques are not valid in the large ρ_i region near the field null. Early computation-intensive ‘hybrid’ models with fluid electrons and kinetic ions showed tilt growth rates decreasing to $\gamma \sim \gamma_{MHD}/10$ when $s = 2$ ($\gamma_{MHD} = V_A/(\ell_s/2)$ where V_A is the Alfvén velocity),[25] which could allow for the FRC lifetimes of ~ 100 μ sec obtained in initial small experiments, but not account for their robustness to dynamic formation or translation, nor for the longer lifetimes of later high s FRCs. Given the computational burden of the hybrid model, a simpler fluid based approach to FLR was developed using Braginskii gyroviscosity.[26] Using a trial-function approach, the tilt mode was found to be stabilized if $S^*/E < 3$. This boundary was occasionally quoted as a stability limit implying that very long FRCs were necessary, even though later LSX FRCs were stable beyond this limit.[27] More sophisticated treatments of the gyroviscous model followed, based on a computation of the actual instability eigenmodes.[28] It was shown that increasing the elongation only improved the stability up to a point, i.e. the so called S^*/E scaling failed. For $E > 3$ the stability boundary ‘leveled-off’ at about $S^* = 10$. At higher elongation the tilt disturbance concentrates in the end regions so that the ‘inertia’ effect associated with larger E no longer increased.

Kinetic effects alone thus do not appear to account for observed FRC stability, although they undoubtedly contribute to the robustness of low s FRCs. Two other effects have been calculated

to contribute to stability. The first is rapid flow, with possibly strong shear. High azimuthal velocities have been measured in all FRCs, and calculations including conservation of generalized helicity (magnetic plus flow) predict high beta minimum energy states (MES) which have both poloidal and azimuthal flows and moderate toroidal fields (as generally seen in FRCs when using internal probes).[29] The other effect is energetic ion components, especially when axis encircling. Such components were calculated in the early 1990s to stabilize the $n=1$ tilt[30]. Recent fully kinetic calculations, including all possible modes, resulted in complete non-linear stability for otherwise unstable oblate FRCs when high energy ion ring components were added.[31] Such calculations are promising enough that a large privately funded experimental program has begun devoted to TNBI sustained FRCs with an ultimate goal of aneutronic fusion.

It has been suggested by some critics that a small, cold (small ρ_i), high density FRC experiment be built solely to test stability at large s . However, it is almost certain that such a highly collisional FRC, without any flow or flow shear, would exhibit the calculated MHD instability. The main hope of realizing the great reactor potential of the simple FRC/FRM geometry is that other effects than standard static MHD will allow FRCs to remain stable at larger sizes, and future experiments should be designed incorporating such effects. As noted in this section, there are many reasons to expect that FRC stability can be extended to higher s values. The s values listed in the Table 1 ‘POP-level’ columns are at about the limits of what has been realized in the pulsed high density LSX experiments, but can be studied in a much more thorough manner without the confusing, and generally irreproducible theta-pinch formation dynamics. The s values can also be increased by a factor of $\sqrt{2}$ simply by using hydrogen instead of deuterium (this will also reduce v_{de}/v_{ti} and yield additional resistivity scaling data). A combination of RMF and TNBI will also provide control of azimuthal velocity profiles and allow studies of flow shear and energetic ion contributions to stability. It is only in this manner that a truly definitive study of stability can be made.

4. FLUX SUSTAINMENT POWER

As previously mentioned, poloidal flux build-up/sustainment in a compact toroid requires making E_θ (Eq. 1) greater than/equal to zero everywhere. Normally, with $\zeta < 1$, the RMF penetration and drive occurs mainly on the outer flux surfaces, and $\langle -V_{ez}B_r \rangle$ exceeds $|\eta_\perp j_\theta|$ there, producing an inward v_r everywhere (it doesn’t matter for current drive whether this is a total radial fluid flow, or just a radial electron flow). It is this inward flow that maintains $E_\theta = 0$ on the inner portion of the FRC, and is the reason why the torque based analysis of Eq. (2) is appropriate. It is also the reason why RMF drive results in low separatrix densities and long particle lifetimes. (Calculation of particle loss out the FRC ends awaits fully 3-D analysis.) Equation (6) gives the results of the torque analysis, and Eq. (8) shows how much RMF power absorption is associated with this process.

It is doubtful that RMF current drive alone would be sufficient as one scales to reactor dimensions. For one thing, the optimal (but not required) RMF frequency scales as $1/r_s^2$, as is evident from Eq. (5). The small Princeton FRC experiment, PFRC, with $r_s \sim 3$ cm utilizes $f_\omega = 14$ MHz,[32] the 20 cm diameter STX (Starthrust Experiment)[33] had $f_\omega = 350$ kHz, and TCSU with $r_s \sim 37$ cm usually is run at $f_\omega = 110$ kHz. Reducing $\omega = 2\pi f_\omega$ still further will result in some azimuthal torque on the ions, making RMF current drive less efficient. In addition, the azimuthally dependent radial forces exerted by the RMF will be of lower frequency, and could produce undesirable radial oscillations. There are also $j_\theta B_r$ forces which, when at lower frequency, will induce sheared axial motions. (It is possible that these oscillations contribute to stability, but this low frequency RMF regime has not been well explored.) It is possible that, other than for initial startup, RMF will only be used as an auxiliary current drive and stabilization technology for larger FRCs, with tangential neutral beam injection becoming the primary current drive mechanism (as originally proposed for FRMs), with assist in the reactor regime from fueling and the reaction products.

For initial startup to the point where TNBI can become effective, it is necessary that steady-state FRCs be formed with of order 50 mWb of flux (it is actually the $B_e r_s$ product that is critical, but r_s should be of order 1 m for typical 10-cm diameter neutral beams). Under TNBI two new effects will contribute to flux, or current drive. The first is simply the fast ion contribution to the total azimuthal current, which will reduce the bulk azimuthal diamagnetic current which experiences a high η_\perp . The second effect is due to the radial flow resulting from an input dn/dt . If not for the vanishing of the $v_{er} B_z$ drive term at the field null, this particle input, and some accompanying energy input, could alone sustain the configuration.

FRC flux lifetimes have been analyzed in terms of $\eta_\perp j_\theta$ at the field null. For a RR type profile typical of all FRCs formed to date, with $B_z(r) = B_e \tanh K_{RR} u$, $n = n_m \text{sech}^2 K_{RR} u$ with K_{RR} a RR parameter usually between 0.7 (for low x_s FRCs) and 1.5 (for high x_s FRCs) and $u = (r/R)^2 - 1$, the basic unsustained flux lifetime is

$$\tau_\phi \approx \frac{R^2}{8D_\eta} \quad [11]$$

where $D_\eta = (\eta_\perp/\mu_0)$. (The factor of 8 arises partially because the distance between the field null and the separatrix is $0.414R$.) Strong particle addition can increase τ_ϕ substantially by flattening out the $B_z(r)$ profile near the field null, thus reducing the current density there. It is worthwhile to consider the contribution from particle input alone from a global viewpoint, ignoring the singularity at the field null, which is not really describable from a simple fluid model. The question of whether any RMF input would be needed at reactor parameters must be left to a more detailed model. Particle input would certainly reduce the RMF power input requirements, and a global model will give some indication of the extent of this reduction. The v_r required to balance

$\eta_{\perp j_0}$ is $v_r = (\eta_{\perp}/\mu_0)/\ell_b$ where ℓ_b is the scale length of B_z (proportional to R). Using the continuity equation $dn/dt = -(n/r)\partial(rv_r)/\partial r$, the rate of particle input, dn/dt must be proportional to nD_{η}/R^2 . Due to the singularity at the field null the total required input rate cannot be integrated exactly, but in correspondence with the standard FRC flux loss time of τ_{ϕ} we can take the required dn/dt as approximately $8nD_{\eta}/R^2$. Then the total required line input rate to alone maintain the FRC flux is of order

$$\dot{N}_{\ell} \approx 8\pi nD_{\eta} \quad [12]$$

This is a very approximate result, but gives an order of magnitude estimate for the contribution from particle addition. It is interesting that this required particle addition is not dependent on FRC size or temperature, but is, of course, highly dependent on the cross-field plasma resistivity. It thus scales well toward reactor parameters. The effect of particle addition on plasma temperature has not been considered, but any imagined reactor particle addition, either from TNBI or fusion reactions, will also supply extra heating.

Tangential neutral beam addition can also produce a fast ion ring which will contribute to flux build-up and sustainment, as well as stability. The ratio $\alpha_{rb} = I_r/I_b$ of ring to neutral beam current can be quite large at low plasma densities and high temperatures. Detailed calculations of this ratio, including the significance of the critical E_{ic} beam energies listed in Table 1, are given in Section 6. No assumptions need be made here about electron flow cancelling out the beam current since the total FRC line current is determined by ΔB_z which is, in turn, determined by the poloidal flux, which can only change with changes in $E_{\theta}(R)$. Initially, the beam ring current will just replace some of the bulk diamagnetic current, which should lead to an increase in E_{θ} as given by Eq. (1) if the effective resistivity seen by the beam current is less than that of the bulk plasma current.

Although high energy ion contributions from either TNBI or fusion reaction products can contribute significantly to FRC current drive, the value of $D_{\eta} = (\eta_{\perp}/\mu_0)$ is still key. Particle and energy transport will also be related to this flux diffusion parameter. Many theta pinch and FRC experiments have been modeled using a D_{η} value which is strongly dependent on the ratio of electron drift velocity, v_{de} to the ion thermal speed v_{ti} . A lower-hybrid-drift (LHD) formula with an algebraic dependence on $\gamma_d \equiv v_{de}/v_{ti}$ has been very descriptive of theta-pinch results,[34] while an exponential dependence (Chodura) has been used to describe both FRC formation and decay.[21] An expression for LHD turbulence was calculated several decades ago to explain theta-pinch diffusion.[35]

$$D_{LHD} = 0.15D_B \frac{\gamma_d^2}{1 + \frac{\pi}{8}\gamma_d^2} \quad [13]$$

$D_B(\text{m}^2/\text{s}) = T_e(\text{eV})/16B(\text{T})$ is the Bohm diffusion coefficient. Although Eq. (13) strictly applies to electrostatic drift waves in low β plasmas, we will use it for both the FRC low β edge region (where the observed η_{\perp} is highest) and for the electromagnetic type turbulence expected near the field null. It is the scaling with drift parameter that is key.

The values of $D_{\eta} = \langle \eta_{\perp} / \mu_0 \rangle$ for TCSU and TCSU Argon and Deuterium experiments, based on Eq. (6), are plotted in Fig. 4 versus D_B . For the TCSU and TCSU Argon experiments the plasmas were very collisional, with $\ell_s / \lambda_{ii} < 1$, and D_{η} follows Bohm scaling. However, the TCSU Deuterium plasmas were collisionless, $\ell_s / \lambda_{ii} > 1$, and D_{η} follows the D_{LHD} -like scaling of Eq. (13). The electron rotation velocity for a rigid rotor profile is $\omega_{\text{RR}}(\text{rad/s}) = 4K_{\text{RR}}T_i(\text{eV})/B_e(\text{T})R^2(\text{m})$. Using $K_{\text{RR}} = 1.5$ typical of RMF sustained FRCs, $v_{\text{ti}} = (kT_i/m_i)^{1/2}$ (actually closer to the ion sound speed), and the pressure balance relationship $B_e = (2\mu_0kT_in_m)^{1/2}$, the RR drift velocity ratio is

$$\gamma_d \equiv \frac{v_{de}}{v_{ti}} = \frac{0.2A_i^{1/2}}{n_m^{1/2}(10^{20} \text{ m}^{-3})r_s(\text{m})} \left(\frac{r}{r_s} \right). \quad [14]$$

For typical TCSU conditions with $A_i = 2$, $n_m = 1 \times 10^{19} \text{ m}^{-3}$, and $r_s = 0.37 \text{ m}$, $v_{de}/v_{ti} = 2.3(r/r_s)$. A value of 2.3 was used for the D_{LHD} line in Fig. 4. The drift velocity is actually even higher at the edge than for a simple RR distribution since the edge electrons rotate near synchronously with the RMF, while the central $\omega_e < \omega_{\text{RR}}$. This may be the reason why the FRC edge resistivity is seen to be so much higher than the interior resistivity.

The scaling of D_{η} with the drift parameter ratio is key to any FRC/FRM reactor scheme. The D_{LHD} type scaling of Eq. (13) is highly favorable, even better than gyro-Bohm, which only scales linearly with v_{de}/v_{ti} . Temperature is not a factor in the v_{de}/v_{ti} ratio, which scales as $1/Rn^{1/2}$. An experiment to test this scaling should increase $Rn^{1/2}$ by at least a factor of 3, either by making r_s larger or n higher (by increasing B_{ω}). Such a combination is indicated in the POP-level columns of Table 1. The results are likely to be exponentially favorable if η_{\perp} is reduced as expected, and at least the higher temperature and density results should be expected, even without TNBI

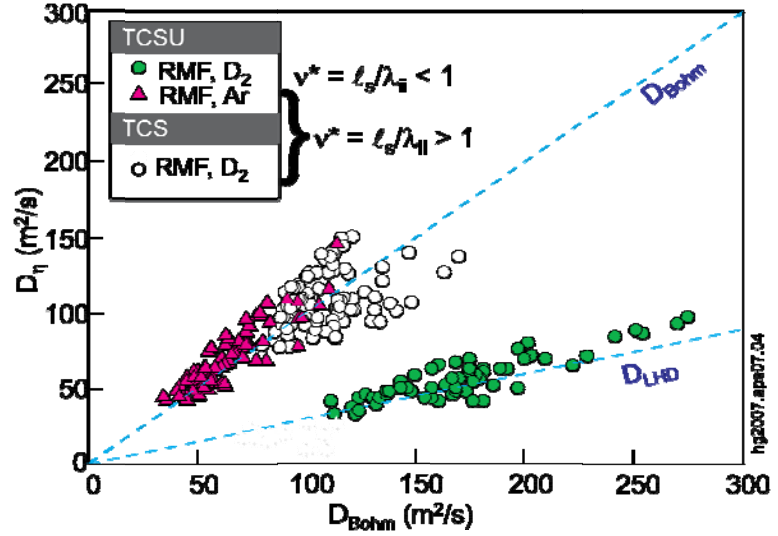


Figure 4. Average effective resistivities in RMF sustained FRCs.

contributions. An idea of what may be possible can be inferred from the high-density theta-pinch formed FRCs (typical LSX low and high field conditions of $n_m = 1.2 \times 10^{21} \text{ m}^{-3}$, $T_e = 175 \text{ eV}$, $T_i = 200 \text{ eV}$, $r_s = 18.5 \text{ cm}$, or $n_m = 1.6 \times 10^{21} \text{ m}^{-3}$, $T_e = 260 \text{ eV}$, $T_i = 570 \text{ eV}$, $r_s = 15 \text{ cm}$ [23]), which had γ_d values of about 0.5. The effective diffusion coefficients obtained from flux decay rates were of order $D_{\perp} \sim 5 \text{ m}^2/\text{sec}$ ($\langle \eta_{\perp} \rangle \sim 6 \text{ } \mu\Omega\text{-m}$), considerably better than necessary to obtain even the second column ‘POP-level’ conditions of Table 1.

Several recent numerical calculations of turbulent diffusion in diamagnetic plasmas exhibit the rapid transition, as implied by Eq. (13), from highly turbulent to near classical diffusion as the drift parameter ratio falls below unity. Loverich and Shumlak observed the development of ion shocks when γ_d exceeded unity in a sophisticated two-fluid code,[36] and similar effects were seen in gyrokinetic calculations by Rogers.[37] Near classical radial confinement was also recently reported in the Gamma-10 tandem mirror facility.[38] If all this experimental and theoretical work is borne out, the great promise of the FRC/FRM approach to fusion would be given a significant boost.

5. ENERGY CONFINEMENT

Energy confinement is the least investigated of all FRC properties because steady state FRCs have not had enough flux to result in more than 1 or 2 ion gyro-radii between the field null and the separatrix. Further, the transport physics in the scrape-off layer is poorly understood since the inferred endloss rates are anomalously slow. Measurements in the Large s Experiment (LSX) were able to account for all energy losses through the sum of radiation and particle losses.[39] It did not appear that any additional losses were occurring through conduction, which is not surprising since the lack of an equilibrium scrape-off layer essentially isolated the plasma inside the separatrix from the boundaries. Analytic calculations for particle loss times were carried out for a full equilibrium FRC where the flux was assumed constant, the temperature uniform, and the scrape-off layer thickness was governed by radial diffusion and axial convection to a specified boundary at the sonic speed. (In the 1-D calculations particle loss was assumed balanced by axial shrinkage.) Numerical results were obtained for a combination of classical and LHD resistivity,[40] and an analytic expression could be obtained for LHD resistivity alone,[41] displayed in somewhat adjusted form below.

$$\tau_p = \frac{R^2}{8D_{LHD}} \left(1 + \frac{3w}{s} \right)^3 \quad [15]$$

In this expression D_{LHD} is approximately based on Eq. (13) taken near the FRC edge, s is the kinetic parameter of Eq. (10), equivalent to a closed field line density scale length divided by the ion gyroradius ρ_{io} in the external magnetic field, and w is the ratio of open field line density scale length to ρ_{io} , always very close to unity. Particle loss in this model is a two step process, first diffusion across the separatrix, and then axial convection. For present low s FRCs open field line

convection is a strong bottleneck, and masks the expected R^4 dependence (since $D_{\text{LHD}} \sim (v_{\text{de}}/v_{\text{ti}})^2 \sim (\rho_{\text{io}}/R)^2$) of LHD transport. The situation should reverse for large s FRCs where closed field line confinement would be expected to dominate, although it may still be possible to influence confinement by restricting the open field line end flow through mirroring or other means.

Energy lifetime can also be thought of as a two-step process in FRCs, especially when the scrape-off layer density is so low that it is in the thermal-flux-limited region where the layer is iso-thermal and energy loss occurs across a sheath where the scrape-off layer encounters a physical boundary. This is a natural occurrence for present RMF sustained FRCs, and may or may not be desirable for larger, more energetic FRCs where the scrape-off layer can be expanded at distant ‘divertors’. The scrape-off power loss is then given by

$$P_{sl} = 4\pi r_s \delta_n \frac{\gamma}{4} p_s \sqrt{\frac{kT_{ts}}{m_i}} \quad [16]$$

where δ_n is the scrape-off layer width, p_s is the separatrix pressure, T_{ts} is the separatrix total temperature, and γ is a sheath parameter usually taken as 8. In numerical terms, for deuterium, with the subscript s signifying the separatrix conditions and m the maximum conditions,

$$P_{sl}(\text{W}) = 2.8 \times 10^4 r_s(\text{m}) \delta_n(\text{cm}) \left(\frac{n_s}{n_m} \right) \left(\frac{T_{ts}}{T_{tm}} \right)^{3/2} n_m (10^{20} \text{m}^{-3}) T_{tm}^{3/2}(\text{eV}) . \quad [17]$$

In typical TCSU plasmas $\delta_n \sim 2$ cm, $n_s/n_m \sim 0.2$, and taking $T_{ts} = T_{tm}$, $P_{sl} = 1.1 \times 10^4 r_s n_m T_{tm}^{3/2}$ using the above units. With $r_s = 0.37$ m, $n_m = 0.1 \times 10^{20} \text{m}^{-3}$, a temperature of $T_{tm} = 180$ eV would produce a value of $P_{sl} = 1$ MW, about half of the absorbed RMF input power in TCSU (with the other half accounted for by radiation). The observed average total temperatures of ~ 200 eV are thus attainable without any internal energy confinement.

Power transfer into the sheath can be described as $P_{\text{Ec}} = E_p/\tau_{\text{Ec}}$, with τ_{Ec} describing both conduction and convection, but not radiation. The plasma energy $E_p = 2\pi R^2 \ell_s \langle \beta \rangle 1.5 n_m k T_{tm}$ and, if we call $\tau_{\text{Ep}} = R^2/4\kappa_{\text{Ec}}$ (dividing by 4 instead of 8 as in τ_ϕ due to losses only occurring across the separatrix), then

$$P_{\text{Ec}} = 12\pi\kappa_{\text{Ec}} \langle \beta \rangle n_m k T_{tm} \ell_s = 600\kappa_{\text{Ec}} (\text{m}^2/\text{s}) \langle \beta \rangle n_m (10^{20} \text{m}^{-3}) \ell_s(\text{m}) T_{tm}(\text{eV}) \text{ W} \quad [18]$$

where κ_{Ec} is a thermal loss diffusion coefficient. For the previous TCSU conditions with $P_{\text{Ec}} = 1$ MW, $\langle \beta \rangle = 0.68$, and $\ell_s = 1.5$ m, this would yield a total temperature $T_{tm} = 164$ eV if $\kappa_{\text{Ec}} = 100 \text{m}^2/\text{s}$. It is thus very reasonable to assume that the low flux TCSU FRCs are isothermal.

For the ‘POP-level’ conditions outlined in Table 1, even with ~ 5 MW power inputs, the scrape-off temperature could not be much over 200 eV if the edge-layer parameters are similar to those seen in TCSU. However, the much higher magnetic flux levels will allow central temperatures to be much higher if κ_{Ec} can be lowered below $25 \text{m}^2/\text{s}$, especially if T_{tm} in Eq. (18)

is taken as the difference between the central and edge temperatures. For reactors, κ_{Ec} would have to be lower than $1 \text{ m}^2/\text{s}$. One objection to using RMF has been that it would open up, at least transiently, all the internal field lines, especially in the absence of any toroidal field. However, calculations by Cohen and Milroy,[42] and later experiments on TCS[43] have shown that by arranging the RMF antennas so that the RMF is in opposite directions in each axial half of the FRC (with both halves rotating in the same direction), the field lines will remain closed. This is an example of innovations which can be brought to this new current drive method. For TCSU size FRCs with so little flux and internal confinement, this innovation is unimportant, but for larger size experiments it may be crucial. Calculations have also shown that this ‘odd-parity’ RMF can preferentially heat different ion or electron species, depending on the frequency, which may find application for both D-T and for advanced aneutronic fuels.[44]

6. TANGENTIAL NEUTRAL BEAM INJECTION (TNBI)

Monte-Carlo calculations have been made for tangential neutral beam injection (TNBI) of deuterium atoms for the ‘POP-level’ and ‘reactor’ cases of Table 1. Assuming a negative magnetic flux inside the field null and positive field outside, the neutral beam is injected at an impact parameter b . The numerical results can best be considered in terms of the characteristic ion energy E_{ic} which, when starting with a tangential velocity $v_\theta = -v_{ic}$ at the field null ($E_{ic} = 0.5m_i v_{ic}^2$), results in an orbit (A) which circles the FRC axis with minimum and maximum excursions equal to R and r_s as sketched in Fig. 5. This characteristic energy[45] is

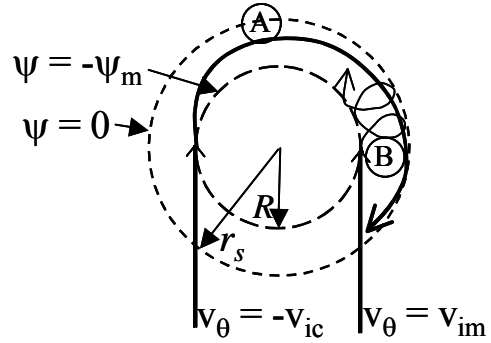


Figure 5. Critical energetic ion orbits in FRCs.

$$E_{ic} \text{ (keV)} = \frac{0.0144}{A_i} \left(\frac{\phi_p \text{ (mWb)}}{r_s \text{ (m)}} \right)^2 \quad [19]$$

and values for the Table 1 cases are listed there for a deuterium beam with $A_i = 2$. Neutral beams injected with higher energies will tend to make excursions outside the separatrix, and be less than ideal for FRC current drive or flux sustainment.

Other possible orbits can be examined by considering the conserved (in the absence of collisions and electric fields) canonical momentum

$$P_\theta = m_i r v_\theta + e\psi \quad [20]$$

and the total kinetic energy

$$H = \frac{m_i}{2} \left(v_r^2 + v_z^2 + \left(\frac{P_\theta - e\psi}{m_i r} \right)^2 \right) \quad [21]$$

For tangential injection and ionization with $v_\theta = -v_b$ and negative ψ , $P_\theta = -(m_i R v_b + e(-\psi))$. (Eq. (19) is derived from calling $H = E_{ic} = m_i v_{ic}^2/2$, calculating P_θ for $v_\theta = -v_{ic}$, $r = R$, and $\psi = -\phi_p/2\pi$, and substituting these values in Eq. (21) for excursions to $\psi = 0$, $r = r_s = \sqrt{2}R$ with $v_r, v_z = 0$.) The maximum radial extent of any orbit can be determined by setting $v_r^2 + v_z^2 = 0$ in Eq. (21), requiring that $\{(-P_\theta) + e\psi\}/m_i r < v_b$. Compared with the characteristic orbit of Fig. 5, for the same $v_b = v_{ic}$ with $b < R$, $(-P_\theta)$ is smaller and ψ can become positive, allowing an orbit excursion outside the separatrix. For $b > R$, $(-P_\theta)$ increases, and the maximum possible ψ is negative (inside the separatrix). If v_b exceeds v_{ic} , $(-P_\theta)$ is again larger, but the above inequality can be satisfied for larger r . Gyro orbits at the separatrix, retro figure-8 orbits, and other possible orbits can be examined with reference to Eqs. (20) and (21). An example (B) with $v_\theta = v_{im}$ and $E_{im} = 0.5m_i v_{im}^2 = E_{ic}/5.8$ is also shown in Fig. 5, which is also typical of bulk ions making retrograde orbits at low s .

The Monte-Carlo calculations of $\alpha_{rb} = I_r/I_b$ can be compared with an ideal estimate assuming that all of the TNBI beam ‘current’ I_b is ionized, captured, and makes axis encircling orbits with gyro time $\tau_g = 2\pi R/v_b$. That would result in a ring current

$$I_r \approx \frac{v_b \tau_s}{2\pi R} I_b \quad [22]$$

where the beam velocity $v_b(\text{m/s}) = 3.1 \times 10^5 (E_b(\text{keV})/A_i)^{1/2}$ and the fast ion slowing down time

$$\tau_s(\text{s}) \approx \frac{0.02}{n_e (10^{20} \text{ m}^{-3})} (T_e(\text{keV}) + 0.27 E_b(\text{MeV}))^{3/2} \quad [23]$$

Ignoring the E_b contribution to τ_s , and taking an average beam velocity of $1.16(E_b/m_i)^{1/2}$ to account for the ion beam time history before thermalizing, the ideal ring to beam current ratio is

$$\alpha_{rb} = \frac{I_{ring}}{I_b} \approx 0.75 \frac{T_e^{3/2}(\text{keV}) E_b^{1/2}(\text{keV})}{A_i^{1/2} n_e (10^{20} \text{ m}^{-3}) R(\text{m})} \text{ kA/A} . \quad [24]$$

This can be compared with the detailed Monte-Carlo calculations, which include ionization, slowing down, and scattering.

From Table 1 it is seen that E_{ic} in TCSU is far too low for TNBI trapping at reasonable beam energies of 10 keV and above. For the first ‘POP-level’ case E_{ic} is 18 keV and for $E_b = 10$ keV in a $B = 60$ mT magnetic field, $\rho_{ic} = 34$ cm. This is an ideal situation since charge-exchange ions can easily remain inside the FRC 90 cm separatrix radius, but also encircle the FRC axis due to the lower magnetic field internal to the separatrix (effective fast ion trap). The fast ion slowing

down time will be of order 10-20 msec, and any planned experiment should provide for timescales of at least that order.

Monte-Carlo calculations have been conducted for various FRC Grad-Shafranov equilibria (with, typical of most FRCs, $\ell_s \sim 5r_s$) to determine α_{rb} ratios. Results are shown by the solid line in Fig. 6 for the first ‘POP-level’ parameters of Table 1 as a function of deuterium beam energy E_b for beam injection along the $b = 0.64$ m ($b = R$) chord. Many particles are tracked, with ionization occurring at various points along the chord, yielding different initial values of v_θ , v_r and v_z .

Since scattering is included in these calculations, the orbits change from ideal paths, and some ions will make excursions outside the separatrix even with $E_b < E_{ic}$. For the $b = R$ injection about 2/3 of the neutral beam was ionized (see Fig. 9). The vacuum tube wall was specified as $r_c = 1.0$ m ($x_s = 0.9$) and beams with energies much beyond E_{ic} produced ions that increasingly intersected the wall, producing decreasing ratios of ring to beam current. This could be alleviated by having the wall further away (not ideal for RMF operation) as shown by the dashed $x_s = 0.8$ curve in Fig. 6, but this is only effective if the neutral density outside the separatrix is low since the fast ions will rapidly charge-exchange with neutrals and be lost. The dash-dotted curve in Fig. 6 shows the effect of 1% neutrals ($n_n = 1.4 \times 10^{17} \text{ m}^{-3}$) outside the separatrix. The ion-neutral charge-exchange cross-section is about $8 \times 10^{-20} \text{ m}^2$, giving a mean free path of about 100 m. For a 20 keV ion travelling at $\sim 10^6$ m/s, the slowing down time (Eq. 23) is about 25 msec, so it normally would travel about 25,000 m. The average distance ions which are lost to charge exchange with the outside neutrals travel is only 2,500 m (~ 100 m of which is outside the separatrix), which accounts for the large reduction in ring current generation. It is thus desirable to keep the neutral beam energy less than $E_{ic}/2$, especially when considering some neutral penetration inside the separatrix.

Ideal curves based on Eq. (24) are shown in all $\alpha_{rb}(E_b)$ figures by dotted lines. For $E_b = 20$ keV in Fig. 6 the ideal α_{rb} is 4.5 kA/A, or 3 kA/A when considering that only 2/3 of the neutral beam is ionized. The Monte-Carlo calculated $\alpha_{rb} = 2.5$ kA/A value in Fig. 6 reflects more realistic orbits. Equation (24), adjusted for TNBI ‘shine-through’, can be used for approximate scaling analysis. It is also important that the beam energy exceed the electron temperature by about a factor of 50, or the slowing down time will be reduced due to collisions with ions. This will be seen to be a factor at higher electron temperatures.

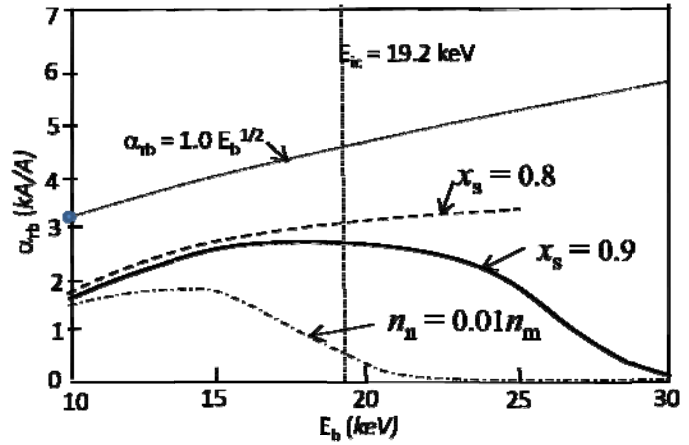


Figure 6. TNBI efficiency for 60 mT FRC with $b = 0.64$ m.

The dependence on injection position is shown in **Fig. 7**. It is slightly more advantageous to inject at $b > R$ since the average canonical angular momentum ($-P_\theta$) will be larger, but for the Figs. 6,7 conditions this is compensated by a lower fraction of the beam being ionized. Such effects depend on the density-length product, but injecting with b between R and $1.15R$ ($\Delta b \sim 10$ cm for the proposed ‘POP’ conditions) is probably optimal for most TNBI scenarios.

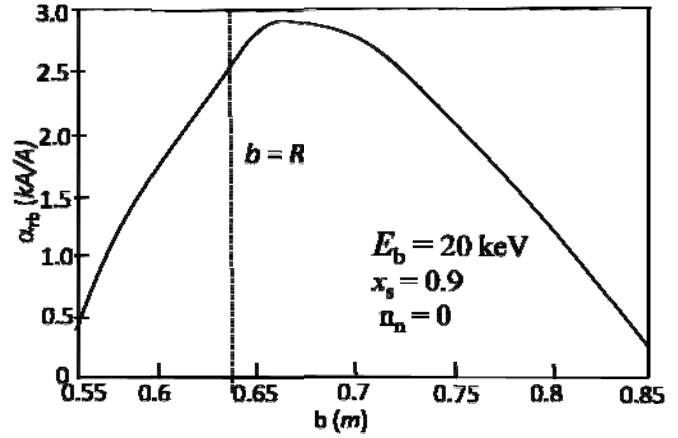


Figure 7. TNBI efficiency for 60 mT FRC as a function of impact parameter.

The ring to beam current ratio for the second column of the ‘POP-level’ parameters is shown in **Fig. 8**. Now E_{ic} is much larger and higher beam energies can be accommodated. Eq. (24) gives an accurate result for an 80 keV neutral beam because the ionization fraction is much higher at the second column density. The percent ionization of the neutral beam is shown in **Fig. 9** for three different conditions. The dotted line in Fig. 8 is the ideal scaling proportional to $E_b^{1/2}$, and the actual results are lower than this scaling at lower beam energies primarily due to slowing down on ions starting to contribute.

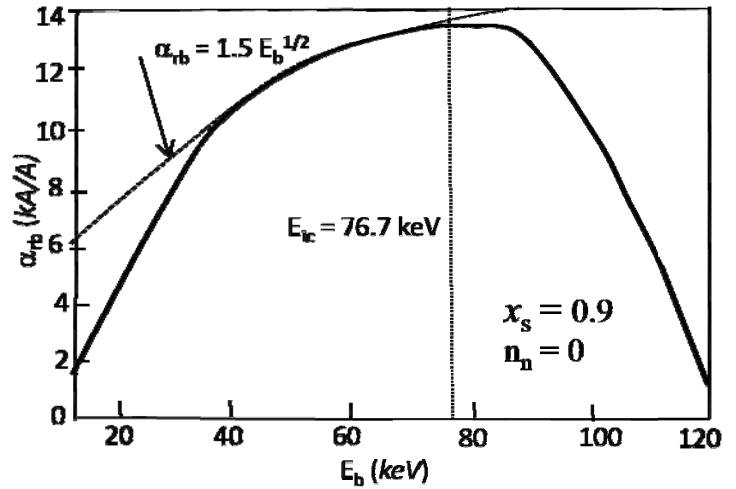


Figure 8. TNBI efficiency for 120 mT FRC with $b = 0.64$ m.

From Eq. (19) it is evident that it is not the flux, but the $r_s B_e$ product which determines E_{ic} . It would thus be possible to obtain the same E_{ic} by doubling B_e in a half-sized device. If the temperature remained the same, the density would quadruple, which in this range would be helpful in increasing the beam ionization fraction, but result in much lower α_{rb} values due to the factor of four decrease in beam slowing down time. However, Eq. (7) shows that the RMF produced ratio of B_e/B_ω would decrease, requiring a more than doubling of RMF B_ω assuming the resistivity remained constant (since $\gamma_d \propto 1/r_s n_m^{1/2}$ is unchanged). The neutral beam profile would have to have a diameter of about 5 cm, instead of 10 cm for the 0.9 m separatrix radius

case. The conditions given in Table 1 are thus probably optimal for TNBI experiments on RMF sustained FRCs. Previous calculations showed that the RMF itself would not greatly reduce the ring current provided that it did not penetrate too far into the plasma [45], but electric fields will have some effect and should be considered in more advanced calculations.

The critical beam energy E_{ic} is very large for the ‘reactor’ conditions of Table 1. A 2 MeV deuterium ion has a gyro orbit of only 22 cm in a 1.3 T magnetic field, far smaller than the 1.41 m field null radius, and most ionization occurs well outside the field null due to short ionization path lengths at the $2 \times 10^{20} \text{ m}^{-3}$ peak reactor condition density. The current drive efficiency can still be quite large, however, even though the energetic ion orbits will be far more complex than the type illustrated in Fig. 5 (more like the retro-orbits shown there, but in the current-carrying direction). The main obstacle at the higher density reactor conditions would be achieving sufficient neutral beam penetration. Ring to beam current ratios are shown by the open circles in Fig. 10, and compared with the Eq. (24) ideal scaling of $\alpha_{rb} = 187 E_n^{1/2} (\text{MeV})$. In contrast

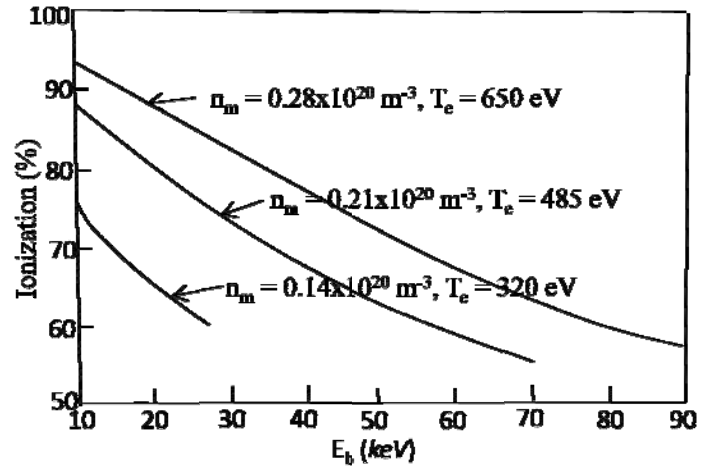


Figure 9. Ionization fraction with $b = 0.64 \text{ m}$.

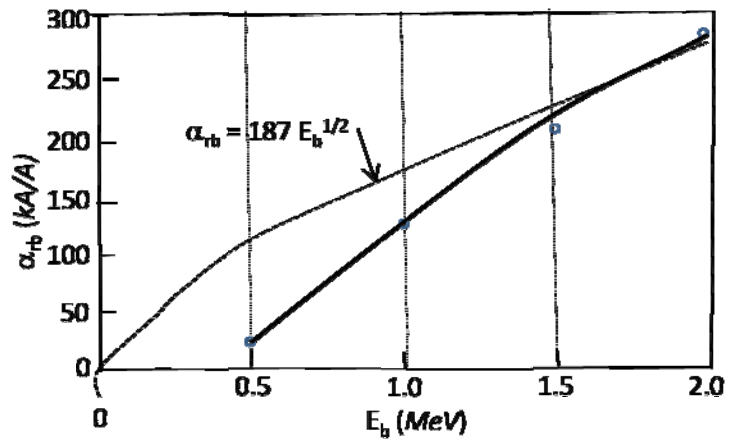


Figure 10. TNBI efficiency for 1.3 T FRC with $b = 1.44 \text{ m}$.

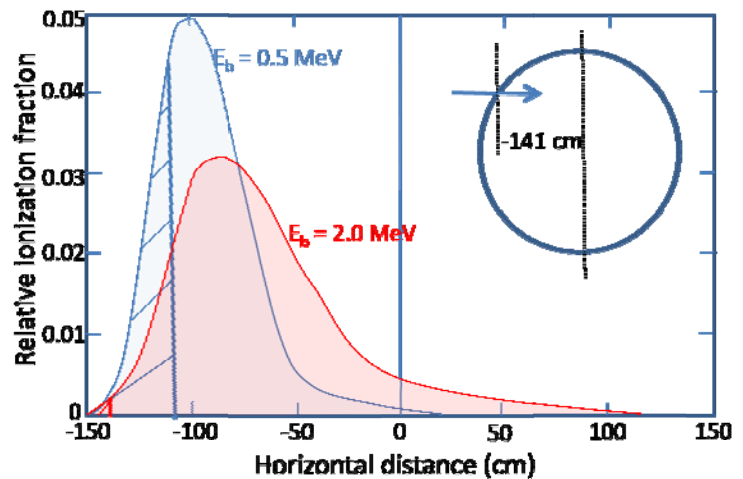


Figure 11. TNBI penetration for 1.3 T FRC with $b = 1.44 \text{ m}$.

to TNBI for the low density conditions where ‘shine-through’ can be a problem, lack of penetration at the higher density ‘reactor’ conditions can lead to poor current drive performance. This is illustrated by the calculations shown in **Fig. 11** of the fractional neutral beam ionization position for two beam energies. Ideally, one would like the beam to penetrate to a horizontal position of 0 (the field null), which doesn’t occur for either of the two beam energies shown. Atoms ionized in the hatched areas to the left of the bold vertical lines actually produce energetic ion orbits in the counter-current direction. The large percentage of atoms being ionized there at $E_b = 0.5$ MeV accounts for the poor performance seen in Fig. 10 at beam energies below 1 MeV. It might be desirable for such conditions to inject at a different impact parameter.

Calculations have also been made of the alpha particle deposition for the ‘reactor’ case, and their contribution to current drive. Current drive will occur due to both the outward alpha particle diffusion, and their tendency to orbit in the current carrying direction despite isotropic birth velocities. Unfortunately both effects are fairly small, although their contributions near the field null could have special importance. For the Table 1 ‘reactor conditions’ with a 10-m FRC length and 90 m³ volume, the alpha production is 16.5 MW, of which 12.2 MW (74%) is deposited in the FRC (10 MW to electrons and 2.2 MW to ions). The rest of the alpha power is lost out the ends. Magnetic mirrors added at both ends improve the axial particle confinement and increase the deposited alpha energy fraction to 86%. The generated alpha particle current is 0.2 MA, far less than the 16.4 MA total equilibrium toroidal current. If one considered the 1.8×10^{20} s⁻¹ alpha generation rate as a 29 amp current, the current generation efficiency would only be 7 kA/A. TNBI is a much more efficient means of generating fast ion currents. The alpha generation rate can contribute to sustaining the FRC through diamagnetism according to Eq. (12), if the resistive diffusion coefficient is very small.

For the Table 1 ‘reactor’ conditions (with a 10 m FRC length) the total plasma energy is only 42 MJ, and the required energy confinement time based on alpha heating alone would be 3.5 sec (2.9 sec with mirrors). An energy transport parameter based on $\tau_{Ec} = R^2/4\kappa_{Ec}$ is $\kappa_{Ec} = 0.14$ m²/sec. Higher κ_{Ec} values could be tolerated by making the FRC larger or higher density. However, the TNBI current drive efficiency would then decrease substantially unless the beam energy was raised beyond 1 MeV. For example, doubling the FRC density results in α_{rb} decreasing from 143 to 40 kA/A for 1 MeV beam energies. If TNBI were to be used alone as a current drive methodology for FRCs, large size, lower density operation would be favored unless higher neutral beam energies were available.

7. SUMMARY

The experimentally demonstrated ability to form and sustain the flux in FRCs using rotating magnetic fields (RMF) has reopened the possibility of realizing the reactor benefits of the old

field reversed mirror (FRM) concept. The primary concern about this concept, stability at larger dimensions, is being addressed by inclusion of many non-standard MHD effects such as strong sheared flow (with small, naturally arising, toroidal field components), and fast energetic ion components (which can arise from both TNBI and RMF drive). Energetic ion rings have been calculated to be able to provide stability to otherwise numerically unstable FRCs, and a large private effort is devoted to purely TNBI sustained FRCs. Independent of the ratio of ring to plasma current needed to provide FRC stability, efficient flux sustainment will still require low cross-field resistivities $\eta_{\perp} \sim 1 \mu\Omega\text{-m}$ ($D_{\perp} = \eta_{\perp}/\mu_0 \sim 1 \text{ m}^2/\text{s}$) and equivalently low, possibly related, thermal diffusion. (Higher η_{\perp} values are tolerable if the ring current is a substantial portion of the bulk plasma current.) Present experiments have average $\langle\eta_{\perp}\rangle$ values of about $100 \mu\Omega\text{-m}$ and κ_{Ec} has yet to be measured. The realization of an efficient FRM reactor requires, at least, that the present high anomalous resistivity decreases with reductions in the drift parameter ratio $\gamma_d = v_{de}/v_{ti}$ to well below unity. Both high density theta-pinch FRC experiments and recent sophisticated numerical calculations give evidence for such an occurrence. Examples are shown in this paper of how γ_d values below unity can be achieved with modest extensions of present RMF facilities. These experiments would also be large enough, and have enough flux to effectively utilize tangential neutral beam injection (TNBI) and study stability and energy confinement in a more MHD relevant (higher s) regime. TNBI calculations are also given for reactor relevant parameters (confinement fields as low as 1.3 T). For TNBI to be useful in reactors it is desirable to keep the plasma density low ($\sim 2 \times 10^{20} \text{ m}^{-3}$), but beam energies of order 1 MeV will still be required. If higher magnetic fields are to be used, it is more desirable to raise the plasma temperatures than the plasma densities, from the point of view of both RMF and TNBI current drive.

ACKNOWLEDGEMENTS

This work was supported by the U.S. Department of Energy. The authors thank Houyang Guo and the RPPL team for conducting the TCS and TCSU experiments, and supplying much of the RMF data and figures used in this paper.

REFERENCES

1. N.C. Christofilos, in “*Peaceful use of atomic energy*” (Proc. 2nd Int. Conf., Geneva 1958) Vol. 32, U.N., New York (1958) 279.
2. G.A. Carlson, et. al., “Conceptual design of the FRM reactor”, Lawrence Livermore Laboratory Report UCRL-52467 (May 19, 1978).
3. R.F. Post, “*Mirror approach to fusion*”, Nucl. Fusion **27**, 1579 (1987).
4. T. Cho, et., al., “*Observation and control of transverse energy-transport barrier due to formation of an energetic electron layer with sheared $E \times B$ flow*”, Phys. Rev. Lett. **97**, 055001 (2006).
5. D.E. Baldwin, B.G. Logan, “*Improved tandem mirror reactor*”, Phys. Rev. Lett. **43**, 1318 (1979).
6. B.G. Logan, et. al., “*High- β , gas-stabilized, mirror-confined plasma*” Phys. Rev. Lett. **37**, 1468 (1976).
7. H.A. Davis, R.A. Meger, H.H. Fleishmann, “*Generation of field reversing E layers with msec lifetimes*” Phys. Rev. Lett. **37**, 542 (1976).
8. E. Schamilaglu, J.B. Greenly, D.A. Hammer, “*Ion beam propagation in a magnetized plasma*” Phys. Fluids B **5**, 3069 (1993).
9. M. Tuszewski, “*Field reversed configurations*”, Nucl. Fusion **28**, 2033 (1988).
10. H. A. Blevin and P. C. Thonemann, “*Plasma confinement using an alternating magnetic field*”, Nucl. Fusion Suppl. 55 ~1962!.
11. I.R. Jones, “*A review of RMF current drive and the operation of the rotamak as FRC and a ST*”, Phys. Plasmas **6**, 1950 (1999).
12. A.L. Hoffman, H.Y. Guo, J.T. Slough, S.J. Tobin, L.S. Schrank, W.A. Reass, and G.A. Wurden, “*The TCS RMF FRC current drive experiment*”, Fusion Science and Technology **41**, 92 (2002).
13. H. Y. Guo, A. L. Hoffman, and R. D. Milroy, “*RMF current drive of high-temperature FRCs with high zeta scaling*”, Phys. Plasmas **14**, 112502 (2007).
14. H.Y. Guo, A.L. Hoffman, R.D. Milroy, K.E. Miller, and G.R. Votrubeck, “*Stabilization of interchange modes by RMF*”, Phys. Rev. Lett. **94**, 185001 (2005).
15. W. T. Armstrong, R. K. Linford, J. Lipson, D. A. Platts, and E. G. Sherwood, “*Field reversed experiments (FRX) on compact toroids*”, Phys. Fluids **24**, 2068 (1981).
16. A.L. Hoffman, H.Y. Guo, K.E. Miller, R.D. Milroy, “*Principal physics of RMF current drive of FRCs*”, Phys. Plasmas **13**, 012507 (2006).
17. R.D. Milroy, K.E. Miller, “*Edge driven RMF current drive of FRCs*”, Phys. Plasmas **11**, 633 (2004).
18. S. Ohi, T. Minato, Y. Kawakami, M. Tanjyo, S. Okada, Y. Ito, M. Kako, S. Goto, T. Ishimura, and H. Ito, “*Quadrupole stabilization of the $n=2$ rotational instability of FRC*”, Phys. Rev. Lett. **51**, 1042 (1983).

19. R.D. Milroy, and L.C. Steinhauer, "*Toroidal field stabilization of the rotational instability in FRCs*", Phys. Plasmas **15**, 022508 (2008).
20. M.N. Rosenbluth, M.N. Bussac, "*MHD stability of spheromak*", Nucl. Fusion **19**, 489 (1979).
21. R.D. Milroy, J.T. Slough, "*Poloidal flux loss and axial dynamics during the formation of a FRC*", Phys. Fluids **30**, 3566 (1987).
22. H.Y. Guo, A.L. Hoffman, K.E. Miller, L.C. Steinhauer, "*Flux conversion and evidence of relaxation in a high- β plasma formed by high-speed injection into a mirror confinement structure*", Phys. Rev. Lett. **92**, 245001 (2004).
23. A. L. Hoffman, L.N. Carey, E.A. Crawford, D.G. Harding, T.E. DeHart, K.F. McDonald, J. L. McNeil, R.D. Milroy, J.T. Slough, R. Maqueda, G.A. Wurden, "*The large-s FRC experiment*", Fusion Technology **23** 185 (1993).
24. J. T. Slough, A. L. Hoffman, R. D. Milroy, E. A. Crawford, M. Cecik, R. Maqueda, G. A. Wurden, Y. Ito, A. Shiokawa, "*Confinement and stability of plasmas in a FRC*", Phys. Rev. Lett. **69**, 2212(1992).
25. D.C. Barnes, J.L. Schwarzmeier, H.R. Lewis, C.E. Seyler, "*Kinetic tilting stability of FRCs*", Phys. Fluids **29**, 2616 (1986).
26. L. C. Steinhauer, A. Ishida, "*Gyroviscous stability theory with application to the internal tilt mode of a FRC*", Phys. Fluids B **2**, 2422 (1990).
27. N. Iwasawa, A. Ishida, L.C. Steinhauer, "*Tilt mode stability scaling in FRCs with finite Larmor radius effect*", Phys. Plasmas **7**, 931 (2000).
28. N. Iwasawa, A. Ishida, L.C. Steinhauer, "*Ideal MHD stability of static FRCs*", J. Phys. Soc. Jpn. **69**, 451 (2000).
29. L. C. Steinhauer, A. Ishida, "*Relaxation of a two-species magnetofluid and application to finite-beta flowing plasmas*", Phys. Plasmas **5**, 2609 (1998).
30. D. C. Barnes, R. D. Milroy, "*Stabilization of the FRC tilt instability with energetic ion beams*", Phys. Fluids B **3**, 2609 (1991).
31. E.V. Belova, R.C. Davidson, H. Ji, M. Yamada, "*Advances in the numerical modeling of FRCs*", Phys. Plasmas **13**, 056115 (2006).
32. S. A. Cohen, B. Berlinger, C. Brunkhorst, A. Brooks, N. Ferraro, D. P. Lundberg, A. Roach, and A. H. Glasser, "*Formation of collisionless high beta plasmas by odd parity RMF*", Phys. Rev. Lett. **98**, 145002 (2007).
33. J. T. Slough and K. E. Miller, "*Flux generation and sustainment of a FRC with RMF current drive*", Phys. Plasmas **7**, 1945 (2000).
34. P.C. Liewer, R.C. Davidson, "*Sheath broadening by the LHD instability in post implosion theta pinches*", Nucl. Fusion **17**, 85 (1977).
35. R.C. Davidson, N.A. Krall, "*Anomalous transport in high-temperature plasmas with applications to solenoidal fusion systems*" Nucl. Fusion **17**, 1313 (1977).
36. J. Loverich, U. Shumlak, "*Nonlinear full two fluid study of the $m=0$ sausage instabilities in an axisymmetric Z pinch*.", Phys. Plasmas **13**, 082310 (2006).

37. B. Rogers, "Gyrokinetic simulations of plasma turbulence, transport, and zonal flows in a closed field line geometry", Bull. Am. Phys. Soc. **52**, paper GI2-4 99 (Nov. 2007).
38. T. Cho, "High confinement in fusion oriented plasmas with kV-order potential, ion, and electron temperatures with controlled radial turbulent transport in GAMMA 10", Bull. Am. Phys. Soc. **52**, paper GI2-6 100 (Nov. 2007).
39. J. T. Slough, A. L. Hoffman, R. D. Milroy, R. Maqueda, L. C. Steinhauer, "Transport, energy balance, and stability of a large FRC", Phys. Plasmas **2**, 2286 (1995).
40. M. Tuszewski, R.K. Linford, "Particle transport in FRCs", Phys. Fluids **25**, 765 (1982).
41. A.L. Hoffman and R.D. Milroy, "Particle lifetime scaling in FRCs based on LHD resistivity", Phys. Fluids **26**, 3170 (1983).
42. S. A. Cohen and R. D. Milroy, "Maintaining the closed magnetic-field-line topology of an FRC with the addition of static transverse magnetic fields", Phys. Plasmas, **7**, 2539, (2000).
43. H. Y. Guo, A. L. Hoffman, L. C. Steinhauer, "Observations of improved confinement in FRCs sustained by anisymmetric RMF", Phys. Plasmas **12**, 062507 (2005).
44. S. A. Cohen, A. S. Landsman, A. H. Glasser, "Stochastic ion heating in an FRC geometry by RMF", Phys. Plasmas **14**, 072508 (2007).
45. A.F. Lifschitz, R. Farengo, A.L. Hoffman, "Calculations of TNBI current drive efficiency for present moderate flux FRCs", Nucl. Fusion **44**, **1015** (2004).